

Photonic nanojet enhancement of dielectric microcylinders with metallic coating

CHENG-YANG LIU

Department of Mechanical and Electro-Mechanical Engineering, Tamkang University, No. 151, Ying-chuan Road, Tamsui District, New Taipei City, Taiwan

The detailed analysis of localized photonic nanojets generated at the shadow side surfaces of dielectric microcylinders with different metallic coatings illuminated by a plane wave is reported. Using high resolution finite-difference time-domain simulation, we have found that the photonic nanojets have waists smaller than the diffraction limit and power modulation by metallic coatings. The intensity enhancement of nanojets depends on the thickness of different metallic coatings. We have further analyzed the effect of refractive index and diameter upon the focal length of photonic nanojets. The results may provide a new ultra-microscopy technique of using visible light to detect and image nanoscale objectives such as nanoparticles, optical gratings, and single molecules.

(Received September 24, 2012; accepted April 11, 2013)

Keywords: Photonic nanojet, Microcylinder, Power enhancement

1. Introduction

Scattering of light by small particles has been interest for over one hundred years now since the popular derivation of the quasi-analytical solution for a sphere by Mie theory [1]. Recently, a substantial literature has developed regarding the existence, properties, and applications of the photonic nanojet [2-7]. The photonic nanojet is a narrow, high intensity beam that propagates into the background medium from the shadow side surface of a plane wave illuminated dielectric microcylinder. The nanojet can appear for a wide range of the electrical size of the dielectric cylinder if the refractive index contrast relative to the background medium is less than about 2:1. The full width at half maximum of nanojet is between one-third and one-half wavelength in the background medium and is only weakly dependent upon the diameter of the dielectric cylinder. Subwavelength optical resolution has become necessary for nanoscale applications, as a result, the direct applications of the nanojets for sensing, metrology, Raman spectroscopy [8], two-photon fluorescence enhancement [9], optical trapping [10], white-light nanoscope [11], and detection of deeply subwavelength pits in a metal substrate [12] have been discussed. The photonic nanojet can be extended to optical wavelengths for high density data storage.

On the other hand, one of the most interesting properties of the nanojet is that the backscattering of dielectric cylinder from which it emerges can be greatly enhanced by placing nanoparticles within the nanojets [13-17]. The enhancement of backscattering shows a dependence on the location and dimension of the metal nanoparticles. The nanoparticles can be detected when they are approaching a properly designed microcylinder. The detection of light scattering from nanoparticles is usually limited by the weak scattering intensities, because the scattering cross section of a nanoparticle is much

smaller than the incident wavelength. Therefore, it would be critical to reduce this size dependence to improve the detection sensitivity in far field optical systems. Recently, the superenhancement of nanojets generated at the shadow side surfaces of core-shell microcylinders illuminated by a plane wave is presented by the author [18]. The intensity enhancement of nanojet depends strongly on the thickness of gold shell.

In this paper, we theoretically demonstrate the localized photonic nanojets generated at the shadow side surfaces of dielectric microcylinders with different metallic coatings illuminated by a plane wave. Using high resolution finite-difference time-domain (FDTD) simulation, we have found that nanojets have waists smaller than the diffraction limit. The intensity of nanojets can be enhanced or reduced by metallic coating. We have further analyzed the effect of refractive index and diameter upon the focal length of photonic nanojets. This may provide a new ultra-microscopy technique for using visible light to detect and image nanoscale objectives such as nanoparticles, optical gratings, and single molecules. Details of the calculations and discussion of the results will be presented in the remainder of the paper.

2. Numerical method

The FDTD method [19] is a rigorous, accurate numerical method that permits computer-aided design and simulation of the nanojets by microcylinders and microspheres. Recently, author has conducted high-resolution FDTD simulations on electro-optical resonant switching in side-coupled waveguide-cavity photonic crystal systems [20]. Hence, we study the internal and near external field distributions of plane wave illuminated dielectric microcylinders with different metallic coatings by using high-resolution FDTD technique. The calculations were performed by a direct

numerical solution of the time-dependent Maxwell equations based on the Yee-cell numerical schemes. The FDTD algorithm must be modified at the boundaries of the computational domain where suitable numerical absorbing boundary conditions are applied. The perfectly matched layer absorbing boundary condition [21] is used to our FDTD simulations to terminate efficiently the outer boundary of the computational region. The cylinder center is laid out in the x - y plane. The light propagation is along the x axis. The FDTD space steps in the x and y axes are Δx and Δy , respectively. The space lattice has a uniform square cell size of 1 nm for all calculations that is finer than 1/100 of an incident wavelength. The sampling in time is selected to ensure numerical stability of the algorithm. The transverse electric wave propagation is considered in this paper wherein the incident electric field vector is in the propagation plane. The FDTD code is written in MATLAB[®]. The computer used in the simulation is Intel[®] Core i7 and has 24 GB of RAM. The validation of the FDTD program has been reported by comparing with the exact solution for the light scattering of the small spheres and cylinders [22]. A more detailed treatment of the FDTD method is given in [19-21].

3. Photonic nanojet analysis

The high-intensity, narrow photonic nanojet that emerges from the shadow side surface of a plane-wave-illuminated dielectric microcylinder has been reported by several papers [2-17]. These simulations and experiments have shown that the high intensity nanojets can exist in both the internal and near external fields along the incident axis. The location and intensity of the nanojets depend on the diameter of microcylinder and refractive index contrast between the microcylinder and its surrounding medium. To study the nanojet characteristics, it is necessary primarily to define its spatial length and width. Fig. 1 depicts a schematic diagram for the photonic nanojet parameters. The refractive indices of the dielectric microcylinder, metallic coating, and surrounding medium are n_d , n_m , and n_s , respectively.

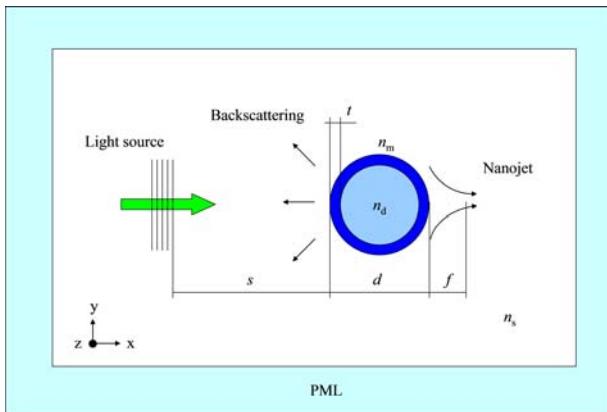


Fig. 1. Schematic diagram for photonic nanojet parameters.

The focal length from the surface of the microcylinder to the point of maximum intensity of the nanojet is f and the distance from the surface of the microcylinder to the plane wave illumination is s . The diameter of cylinder is d and the thickness of metallic coating is t . The refractive indices of the copper and silver coating are $1.02+2.577i$ and $0.06+3.586i$ at the incident wavelength of 532 nm, respectively [22]. The microcylinder is surrounded by air medium ($n_s = 1$).

The FDTD code permits the numerical simulations of the total and scattered fields throughout entire space when an incident lightwave interacts with a core-shell microcylinder. Fig. 2 depicts the focal length as a function of refractive index for dielectric microcylinder with different metallic coatings at $d = 5 \mu\text{m}$. The thickness of metallic coating for copper and silver is $t = 10 \text{ nm}$. At a glance, the focal length reveals some interesting regularities. First, the focal lengths for dielectric microcylinder with and without metallic coating all decrease as refractive index increases. Second, the microcylinders with copper coating have bigger focal length, when the refractive index is in range of 1.7-2.4. The third, the relation between focal length and refractive index became an oscillation curve, when the microcylinder is coated with metals. Fig. 3 shows the normalized power flow patterns of dielectric microcylinders at incident wavelength of 532 nm for different refractive index. It is evident that the internal electric field peak shifts toward the shadow side surface of the microcylinder along the forward direction. The photonic nanojet emerges from the shadow side surface of the microcylinder in Fig. 3(a) as a strong jet-like distribution. The most attractive feature of this nanojet is that it is neither evanescent wave nor optical diffraction. When the refractive index of the core of microcylinder is $n_d = 1.5$, the photonic nanojets have a focal length of 526.3 nm for dielectric cylinder and 674.1 nm for cylinder with copper coating, respectively. In terms of intensity distribution, they all have a waist of about 250 nm. It is smaller than one-half wavelength.

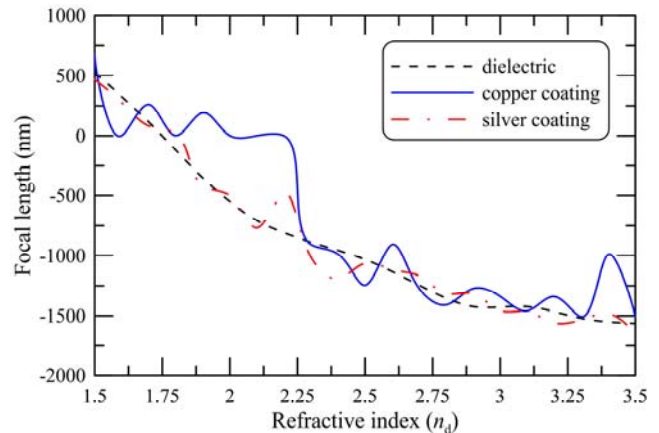
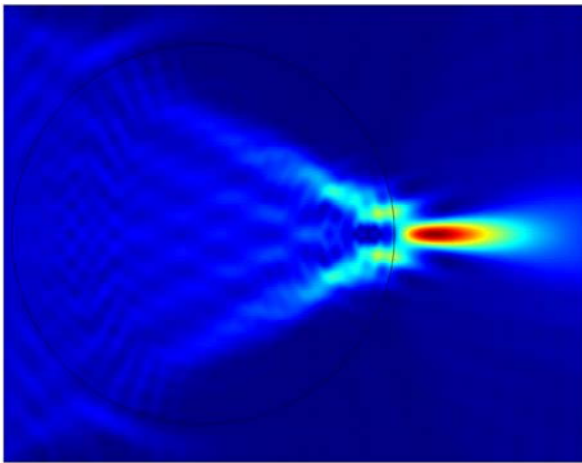
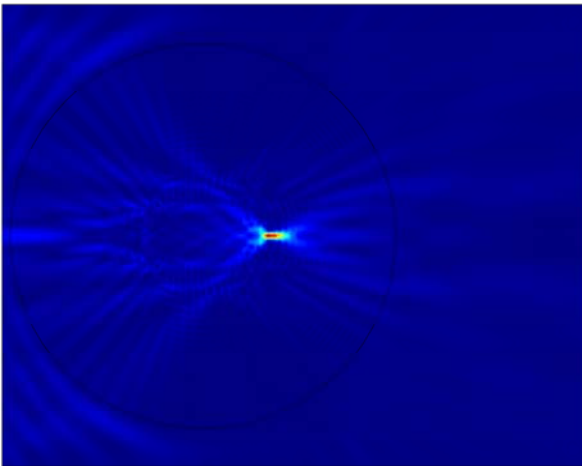


Fig. 2. Focal length as a function of refractive index for dielectric (dashed line), copper coating (solid line), and silver coating (dash-dotted line) microcylinders at $d = 5 \mu\text{m}$ and $t = 10 \text{ nm}$.



(a)



(b)

Fig. 3. Normalized power flow patterns of dielectric microcylinders at refractive index (a) $n_d = 1.5$ and (b) $n_d = 3.5$.

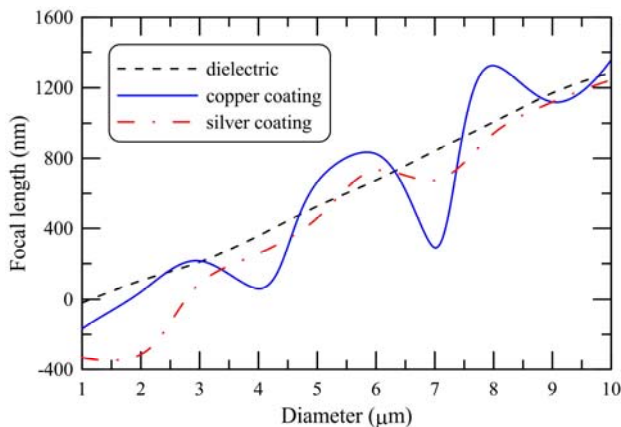
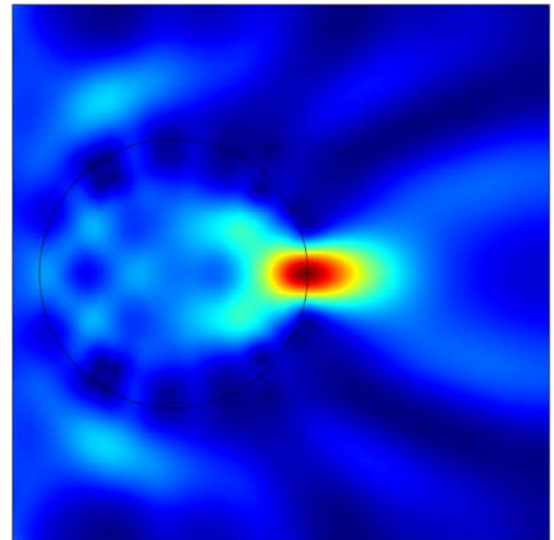


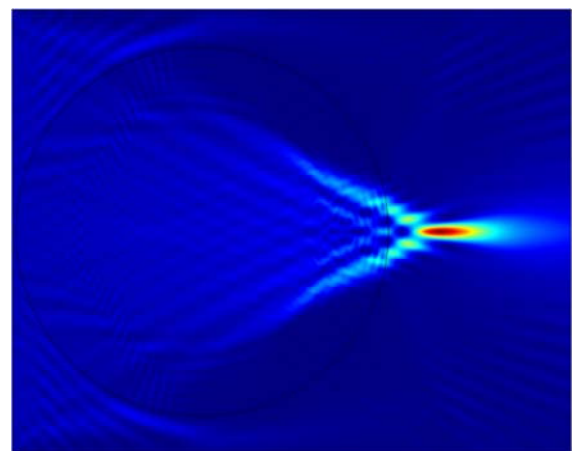
Fig. 4. Focal length as a function of diameter of dielectric (dashed line), copper coating (solid line), and silver coating (dash - dotted line) microcylinders at $n_d = 1.5$ and $t = 10$ nm.

We also discuss the influences of cylinder diameter on focal length of photonic nanojets. Fig. 4 shows focal length as a function of diameter of dielectric

microcylinders with metallic coating at $n_d = 1.5$ and $t = 10$ nm. It can be seen that the focal lengths all increase as cylinder diameter increases. When the diameter of microcylinders is $d = 10 \mu\text{m}$, the focal lengths are 1283.3 nm and 1356.8 nm for dielectric and copper coating cylinder, respectively. Fig. 5 shows the normalized power flow patterns of dielectric microcylinders at incident wavelength of 532 nm for different diameter. For dielectric microcylinder at $d = 1 \mu\text{m}$ in Fig. 5 (a), a photonic nanojet protrudes from the shadow side of microcylinder. As the diameter increases, the nanojet starts to emerge and move away from the microcylinder. The maximum intensity and full-width half-max (FWHM) of the nanojet also increase as the diameter increases. The incident wavelength of 532 nm is chosen as an example. The diameters of microcylinders and the focal length of the photonic nanojets are scalable in respect of the incident wavelength.



(a)



(b)

Fig. 5. Normalized power flow patterns of dielectric microcylinders at diameter (a) $d = 1 \mu\text{m}$ and (b) $d = 10 \mu\text{m}$.

We further discuss the influences of coating thickness on focal length of photonic nanojets. Fig. 6 shows focal length as a function of coating thickness of dielectric, copper coating, and silver coating microcylinders at $d = 5 \mu\text{m}$ and $n_d = 1.5$. In thin coating thickness ($t < 4 \text{ nm}$), the focal length can be extended by silver coating. In thick coating thickness ($4 \text{ nm} < t < 14 \text{ nm}$), the focal length can be dramatically extended by copper coating. The previous studies [13-17] demonstrated a remarkable characteristic of nanojets that nanojets can significantly improve the backscattering by nanoparticles located within the nanojets. In this paper, the metal coating not only extended the focal length but also enhanced or reduced the intensity of nanojets. Fig. 7 shows the intensity profile of nanojets for dielectric microcylinders with metallic coating at $d = 5 \mu\text{m}$ and $n_d = 1.5$. The all intensities of nanojets for microcylinders with different metallic coatings are normalized to the intensity for the dielectric microcylinder. The intensities of photonic nanojet are increased by 20% to 40% for copper coating microcylinders. Fig. 8 shows the normalized power flow patterns of microcylinders with copper and silver coating at $d = 5 \mu\text{m}$ and $t = 10 \text{ nm}$. Comparing Fig. 3(a) with Fig. 8, it is evident that the photonic nanojet intensity of the microcylinder is dramatically enhanced or reduced by the metallic coating. From these studies, we conclude that the focal length of photonic nanojet is effectively controlled by the diameter and refractive index of microcylinder whereas the intensity of photonic nanojet is enhanced or reduced by the metallic coating.

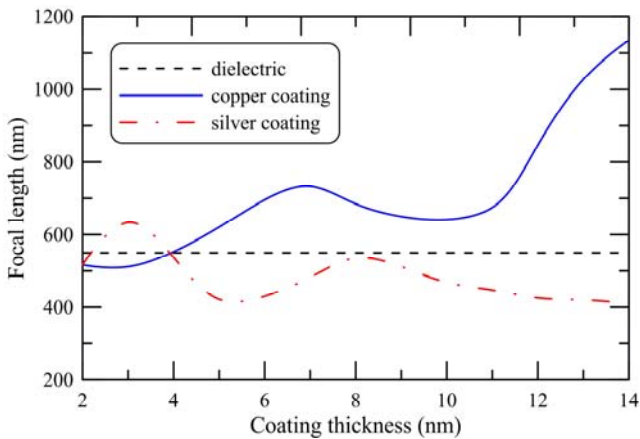


Fig. 6. Focal length as a function of coating thickness of dielectric (dashed line), copper coating (solid line), and silver coating (dash-dotted line) microcylinders at $d = 5 \mu\text{m}$ and $n_d = 1.5$.

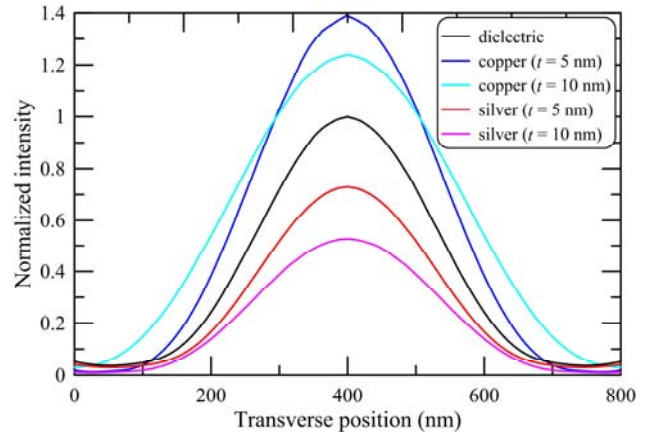
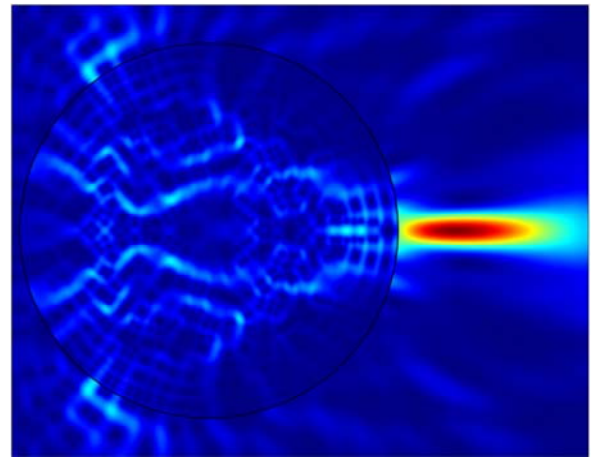
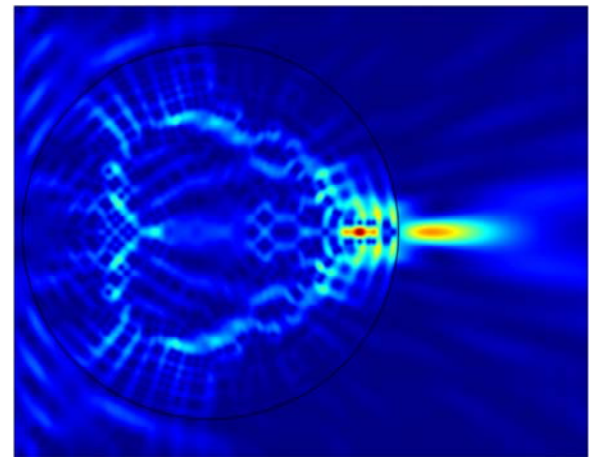


Fig. 7. Intensity profile of photonic nanojet for dielectric microcylinder with metallic coating at $d = 5 \mu\text{m}$ and $n_d = 1.5$.



(a)



(b)

Fig. 8. Normalized power flow patterns of (a) copper coating and (b) silver coating microcylinders at $d = 5 \mu\text{m}$ and $t = 10 \text{ nm}$.

The metallic coating procedures reported in the literature generally involve surfaces with a significant chemical affinity for dielectric material [24-26]. A combination of standard procedures can be used to prepare the dielectric microcylinder with different metallic coatings. The thickness of metallic coating can be varied from a few to several hundred nanometers. Varying the metallic coating thickness and the refractive index of the dielectric cylinder allows control over the optical properties of the dispersions. The metallic coating provides a physical barrier between the optically dielectric core and the surrounding medium that makes a strongly enhanced or reduced optical intensity. The effects of dielectric microcylinder with metallic coating can have a significant impact on biological observation, light emitting devices, and optical microscopy. The backscattering, diffusion, and diffraction studies on these coated dielectric microcylinders are currently being undertaken.

4. Conclusion

We have analyzed numerically the localized nanojets generated at the shadow side surfaces of dielectric microcylinders with different metallic coatings illuminated by a plane wave. Using FDTD simulation, we have found that photonic nanojets have waists smaller than the diffraction limit and power modulation by metallic coatings. The intensity enhancement of photonic nanojets depends on the thickness of metallic coating. We have further analyzed the effect of refractive index and diameter upon the focal length of photonic nanojets. The enhancement of photonic nanojets promises to make a useful application for optical detecting, differentiating, and sorting nanoparticles. By analyzing intensity and distribution of enhanced photonic nanojets from microcylinders with metallic coating, this mechanism could be an important tool in the fields of nanotechnology and nano-biotechnology. Further theoretical investigations and experimental efforts are needed to apply this mechanism in practice.

References

- [1] H. C. Van de Hulst, *Light Scattering by Small Particles*, Dover Publications, New York (1981).
- [2] A. V. Itagi, W. A. Challener, *J. Opt. Soc. Am. A* **22**, 2847 (2005).
- [3] C. Li, G. W. Kattawar, P. Zhai, *Opt. Express* **13**, 4554 (2005).
- [4] P. Ferrand, J. Wenger, A. Devilez, M. Pianta, B. Stout, N. Bonod, E. Popov, H. Rigneault, *Opt. Express* **16**, 6930 (2008).
- [5] A. Devilez, B. Stout, N. Bonod, E. Popov, *Opt. Express* **16**, 14200 (2008).
- [6] K. Holms, B. Hourahine, F. Papoff, *J. Opt. A: Pure Appl. Opt.* **11**, 054009 (2009).
- [7] M. Kim, T. Scharf, S. Mühlig, C. Rockstuhl, H. P. Herzig, *Opt. Express* **19**, 10206 (2011).
- [8] K. J. Yi, Y. F. Lu, Z. Y. Yang, *J. Appl. Phys.* **101**, 063528 (2007).
- [9] S. Lecler, S. Haacke, N. Lecong, O. Crégut, J. Rehspringer, C. Hirlimann, *Opt. Express* **15**, 4935 (2007).
- [10] X. Cui, D. Erni, C. Hafner, *Opt. Express* **16**, 13560 (2008).
- [11] Z. Wang, W. Guo, L. Li, B. Lukyanchuk, A. Khan, Z. Liu, Z. Chen, M. Hong, *Nat. Commun.* **2**, 218 (2011).
- [12] S. Kong, A. Sahakian, A. Taflove, V. Backman, *Opt. Express* **16**, 13713 (2008).
- [13] Z. Chen, A. Taflove, V. Backman, *Opt. Express* **12**, 1214 (2004).
- [14] X. Li, Z. Chen, A. Taflove, V. Backman, *Opt. Express* **13**, 526 (2005).
- [15] Z. Chen, X. Li, A. Taflove, V. Backman, *Appl. Opt.* **45**, 633 (2006).
- [16] A. Heifetz, J. J. Simpson, S. Kong, A. Taflove, V. Backman, *Opt. Express* **15**, 17334 (2007).
- [17] S. Yang, A. Taflove, V. Backman, *Opt. Express* **19**, 7084 (2011).
- [18] C.-Y. Liu, *Phys. Lett. A* **376**, 1856 (2012).
- [19] A. Taflove, S. C. Hagness, *Computational Electrodynamics: The Finite Difference Time Domain Method*, Artech House, Boston (1998).
- [20] C.-Y. Liu, *Phys. Lett. A* **375**, 3895 (2011).
- [21] J.-P. Berenger, *J. Comput. Phys.* **114**, 185 (1994).
- [22] C. Li, G. W. Kattawar, P. Yang, *J. Quant. Spectrosc. Radiat. Transfer* **89**, 123 (2004).
- [23] P. B. Johnson, R. W. Christy, *Phys. Rev. B* **6**, 4370 (1972).
- [24] S. S. Park, B. Y. H. Liu, K. L. Rubow, *Aerosol Sci. Tech.* **16**, 141 (1992).
- [25] L. M. Liz-Marzán, M. Giersig, P. Mulvaney, *Langmuir* **12**, 4329 (1996).
- [26] P. Reiss, M. Protière, L. Li, *Small* **5**, 154 (2009).

*Corresponding author: cyliu@mail.tku.edu.tw